Nuclear Instruments and Methods in Physics Research B 319 (2014) 55–61

Contents lists available at ScienceDirect

Nuclear Instruments and Methods in Physics Research B

journal homepage: www.elsevier.com/locate/nimb

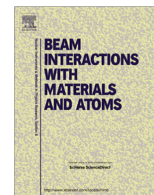

Depth profiling by Raman spectroscopy of high-energy ion irradiated silicon carbide

Xu Wang, Yanwen Zhang, Shiyi Liu, Ziqiang Zhao *

State Key Laboratory of Nuclear Physics and Technology, Institute of Heavy Ion Physics, School of Physics, Peking University, Beijing 100871, China

ARTICLE INFO

Article history:
Received 31 July 2013
Received in revised form 12 October 2013
Available online 1 December 2013

Keywords:
Silicon carbide
Raman spectroscopy
Ion implantation
Damage profile
Strain

ABSTRACT

Single crystals of 6H–SiC were irradiated at room temperature with 20 MeV carbon ions at fluences of 1.5×10^{15} and 6.0×10^{15} cm^{-2}. Raman measurements were performed to study irradiation induced damage and the in-depth damage profile of SiC. A clear change of damage from the surface down to the stopping region of carbon ions as simulated by SRIM is exhibited. The affected area as detected by Raman is in good agreement with SRIM predictions while a little shallower dpa profile is observed. The partial disorder defined in the present work as a function of depth is demonstrated. A shift of the position of the TO peak towards lower wavenumbers with in-depth damage and then to higher wavenumbers beyond the most damaged region indicates that tensile strain due to defects has a backward V-curve distribution. The damaged layer is subjected to a compressive in-plane stress associated with the out-of-plane strain and the magnitude of this stress also has a backward V-curve depth profile. The evolution of line width of the TO peak with depth clearly shows the density of defects reaches the higher level at the most damaged region. The Raman spectroscopy scanning technique is proved to be a powerful tool for profiling of crystal damage induced by high-energy ion implantation.

© 2013 Elsevier B.V. All rights reserved.

1. Introduction

Being considered as a key engineering material in nuclear applications, silicon carbide (SiC) has been the subject of both extensive fundamental studies and practical applications in recent decades [1]. In future GEN IV reactors, especially in the very high temperature gas cooled nuclear reactors (VHTR), SiC has been proposed as a cladding material and/or structural material for the reactor core on account of its excellent properties such as high thermal conductivity, extremely high hardness, chemical inertness and small neutron capture cross-section. In addition, SiC can also be used as an inert matrix for the transmutation of nuclear wastes like actinides [1,2]. However, SiC can readily become amorphous due to ion irradiation induced damage. The damage accumulation and the potential amorphous states have been studied by experimental and theoretical methods [3–13]. The damage, usually represented in dpa (displacement per atom), varies with depth and is higher in the nuclear interaction region, where optical absorption centers related to elastic collisions are formed [14]. Thus, investigation of irradiation induced damage profile is an interesting topic for the understanding of damage accumulation and recovery of the irradiation induced disorder [15–17].

Recently, spectroscopic signatures of ion irradiation induced damage in silicon carbide are of high interest. Raman spectroscopy is a sensitive and non-destructive method to detect different chemical states in materials, including ion irradiated SiC without exception [14,17–21]. In fact, the depth probed by Raman spectroscopy varies with the quality of samples, laser wavelengths and the damage level. As the number of dpa increases, the wafers could become very opaque and the Raman penetration depth decreases drastically, from several micrometers to a few hundreds of nanometers or even less, thus the confocal microscopy technique becomes less efficient for the deeper parts. Though reliable data of the whole sample can be collected when the laser beam is focused on the sample surface rather than some depth underneath, the detailed in-depth damage profile cannot be acquired. Raman spectroscopy scanning technique has been successfully applied for in-depth determination of radiation damage in $Gd_2Ti_2O_7$ single crystals [22]. Moreover, G. Guimbretière et al. determined by Raman spectroscopy the in-depth profile in UO_2 ceramic submitted to 25 MeV He ion irradiation [18]. A clear increase of the damage from the surface up to the position of the implanted He is exhibited and Raman has been proven an excellent way of studying the evolution of defects bands and changes in the T_{2g} peak of UO_2 as a function of implantation depth.

The aim of the present work is to study the damage profile of light ions implanted in SiC and compare the results with SRIM predictions. Furthermore, we tried to qualitatively investigate the

* Corresponding author. Tel: +86 10 62755363.
E-mail address: zqzhao@pku.edu.cn (Z. Zhao).

0168-583X/$ - see front matter © 2013 Elsevier B.V. All rights reserved.
http://dx.doi.org/10.1016/j.nimb.2013.10.017

strain/stress build-up as a consequence of ion implantation. In the present paper, an energy of 20 MeV C ions was chosen so that two distinct damage regions in a depth of about 10 μm can be obtained for convenience. The in-depth disorder profile is investigated under the condition of all measurements taken with the laser beam focused on the surface of a specifically prepared transverse cross section sample.

2. Experimental

2.1. Material and irradiations

350 μm thick (0001)-oriented *n*-type single crystalline 6H–SiC wafers with dimensions of 5×5 mm^2 purchased at Shanghai Institute of Optics and Mechanics, Chinese Academy of Sciences have been irradiated. These single crystal wafers were polished along the *x*–*y* plane and both of the *x*–*z* planes to obtain mirror-like surfaces. Reference axes *x*, *y* and *z* are fixed in the wafer with *z* along the *c*-axis, i.e. $z = (0001)$, *y* perpendicular to one of the polished transverse side, or $y = (100)$ and *x* the other, or $x = (010)$, as is shown in Fig. 1(b). The specimens were irradiated at room temperature under 5×10^{-5} Pa vacuum in order to avoid oxidation, with 20 MeV C^{3+} ions produced by the 2×6 MV tandem accelerator at Peking University. The ion fluences were 1.5×10^{15} cm^{-2} and 6.0×10^{15} cm^{-2}, respectively. Taking the threshold displacement energies for C and Si sublattices as 20 eV and 35 eV respectively [23], the damage was 0.2 and 0.8 dpa at the damage peak. Samples were tilted by 7° in order to minimize channeling effects. Two samples were reconstituted with both *x*–*z* planes face to face, for the sake of reducing the radiative losses from the surface during irradiation [18]. Fig. 1(a) shows the scanning electron microscope picture taken on the *x*–*z* plane of the implanted region in the crystal irradiated at a fluence of 6.0×10^{15} cm^{-2}. We can see a black band corresponding to the most damaged region. The electronic (S_e) and nuclear (S_n) stopping powers for 20 MeV C ions as a function of depth are drawn in Fig. 2(a). The depth distribution of C ions and dpa profile (for a fluence of 1.5×10^{15} cm^{-2}) according to SRIM Monte Carlo calculations [24] are also shown (Fig. 2(b)). The curves related to 20 MeV Au ions are added for the sake of comparison (10^{14} cm^{-2}).

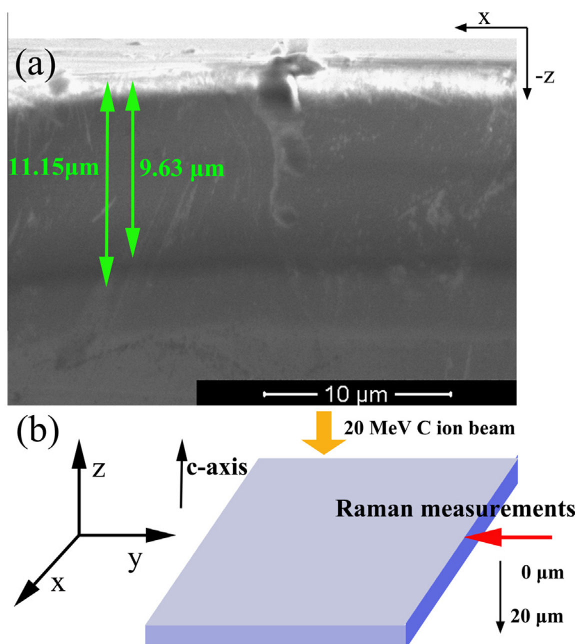

Fig. 1. SEM picture taken on the transverse cross section of the implanted region in the SiC crystal for highest damaged sample (a) and the geometry of irradiation and Raman line scan of the irradiated samples (b).

2.2. Raman configuration

Raman spectra were acquired using the excitation wavelength of 532 nm and a 1800 groove/mm grating (Horiba J.Y. LabRAM ARAMIS), with a scanning range of 600 cm^{-1}–1200 cm^{-1} at a spectral resolution of 0.8 cm^{-1}. A 100 × objective with numerical aperture of 0.9 was employed, which gives spatial resolution better than 1 μm and the sample analyzed volume is on the order of 1 μm^3. The power of the laser light obtained on the sample was about 3 mW. These spectra were acquired starting from 0 μm up to 20 μm with a step of 0.5 μm on the *x*–*z* planes. Actually, to make the boundary '0' μm as accurate as possible, the Raman line scan measurements began from about 3 μm away from the boundary, or at a position of −3 μm. The collected signal will be the largest when the laser spot overlaps with the bulk and this is where '0' μm is defined in the present work. All measurements were conducted at room temperature with the laser beam focused on the surface. This cross-sectional measurement is conducive to overcoming the difficulty of comparing spectra acquired at different depths in confocal Raman mode when samples are too much damaged. The 20 μm range can cover both less distorted and strongly damaged regions as well as unaffected crystallized zone in the irradiated samples according to SRIM calculations. To analyze the Raman spectra, Lorentzians were used to fit the phonon peaks.

Before the spectra are analyzed, we would like to emphasize that Raman characteristics are different taking the anisotropy of Raman scattering in 6H–SiC into consideration, which has been reported in several papers [25–28]. The anisotropy of the phonon dispersion is taken into account for the shift of phonon modes due to defects and the anisotropy should be distinguished [27]. The bond polarizability model has been used to calculate the Raman intensities of folded modes in the transverse optical and acoustic branches [26]. Raman active modes of A_1, E_1 and E_2 symmetry are allowed in 6H–SiC, which has a wurtzite structure with C_{6V}^4 space group. The A_1 and E_1 symmetry phonon modes are both Raman and IR active and they split into longitudinal and transverse branches, while the E_2 mode is infrared inactive. However, different Raman scattering intensities, peaks splitting and some peaks emerging or missing are depending on the specific Raman measurement configuration. Table 1 shows Raman frequencies of the folded modes and assignment for the first-order peaks of 6H–SiC. Note that Raman peaks and the attribution are different when a-plane is used for two different backscattering geometries. The differences of details of these Raman spectra are due to the direction of the laser and crystal orientations. The Raman configuration used in the present work was $y(z, x+z)y$. The first and last letters in $y(z, x+z)y$ denote the direction of incident laser light and scattered light, respectively. The letters given in the bracket are the polarization of incident and detected light respectively. This symbol means that only the incident light is polarized and no polarizer was used in the scattered beam in our measurements. Herein, only E_1 and A_1 modes are allowed for the -zx- and -zz- polarization components respectively and the E_2 modes are not allowed, as displayed in Table 1. In a nutshell, different geometries can be used when disorder profile is studied using Raman spectroscopy.

3. Results and discussion

3.1. In-depth damage analysis

The amorphization mechanism is strongly related to the energy of ions and the ion mass, which can influence the Raman

Download English Version:

https://daneshyari.com/en/article/8041989

Download Persian Version:

https://daneshyari.com/article/8041989

Daneshyari.com